Posted on 26 Aug 2024 | The copyright holder is the author/funder. All rights reserved. No reuse without permission. | https://doi.org/10.22541/au.172471102.26164569/v1 | This is a preprint and has not been peer-reviewed. Data may be preliminary.

Continuous stem water potential measurements of a diffuse-porous tree species offer new insights into tree water relations

Simon Haberstroh[1], Fabio Scarpa[1], Stefan Seeger[2], Andreas Christen[1], and Christiane Werner[1]

[1]Albert-Ludwigs-Universitat Freiburg Fakultat fur Umwelt und Naturliche Ressourcen
[2]Georg-August-Universitat Gottingen Department fur Nutzpflanzenwissenschaften

August 26, 2024

Abstract

Water potential is a crucial parameter for assessing tree water status and hydraulic strategies. However, methods for measuring water potential, such as the Scholander pressure chamber, are destructive and discontinuous, and difficult to perform in tall forests. Consequently, important dynamics in water potentials, particularly during short-term drought, are difficult to capture. Recent advancements have introduced low-maintenance sensors capable of measuring continuous, high-resolution stem water potentials. If applicable to forest trees, such sensors hold the potential to significantly enhance our understanding of tree water relations. We evaluated these sensors in a temperate, diffuse-porous tree species (*Carpinus betulus*) over a growing season marked by dry-down periods and heat. Concurrent measurements of branch water potential, sap flow, and environmental factors (air temperature, vapor pressure deficit, and soil water content) were conducted. Midday stem water potentials of *C. betulus* reached minimum values of -3.39 ± 0.10 MPa and exhibited pronounced seasonal fluctuations, mirroring changes in environmental conditions and sap flow. Comparison of stem water potentials with Scholander-type measurements revealed a very good correlation with predawn ($R^2 = 0.98$) and a general agreement with midday measurements ($R^2 = 0.71$). Diurnal variations in stem water potentials and sap flow exhibited a hysteresis, consistent with other plant parameters. In this first assessment, the agreement with Scholander-type measurements, sap flow, and environmental parameters suggests the tested water potential sensors yield reliable data. If applicable to other tree species, including conifers, these sensors could significantly advance our understanding of tree water relations and their role in forest drought responses.

Continuous stem water potential measurements of a diffuse-porous tree species offer new insights into tree water relations

Simon Haberstroh[1], Fabio Scarpa[1], Stefan Seeger[2], Andreas Christen[3], Christiane Werner[1]

[1]Ecosystem Physiology, Faculty of Environment and Natural Resources, University Freiburg, Freiburg, Germany

[2]Soil Physics, Department of Crop Sciences, University of Göttingen, Göttingen, Germany

[3]Environmental Meteorology, Faculty of Environment and Natural Resources, University Freiburg, Freiburg, Germany

*corresponding author: simon.haberstroh@cep.uni-freiburg.de, +49 761 203 8303, ORCID: 0000-0002-6097-6633

Keywords

Carpinus betulus , midday water potential, predawn water potential, sap flow

Posted on 26 Aug 2024 | The copyright holder is the author/funder. All rights reserved. No reuse without permission. | https://doi.org/10.22541/au.172471102.26164569/v1 | This is a preprint and has not been peer-reviewed. Data may be preliminary.

Acknowledgements

We thank Thomas Plapp, Dirk Redepennig, Dirk Schindler and Matthias Zeeman (Chair of Environmental Meteorology, University of Freiburg) and Thomas Seifert, Benjamin Gebert (Chair of Forest Growth and Dendroecology, University of Freiburg) for site logistics data management, and support. We acknowledge funding of the SFB1537 (ECOSENSE) (Werner et al., 2024) and support by the Integrated Carbon Observation System (ICOS, Site DE-Har) for processing and managing the long-term environmental data.

Abstract

Water potential is a crucial parameter for assessing tree water status and hydraulic strategies. However, methods for measuring water potential, such as the Scholander pressure chamber, are destructive and discontinuous, and difficult to perform in tall forests. Consequently, important dynamics in water potentials, particularly during short-term drought, are difficult to capture. Recent advancements have introduced low-maintenance sensors capable of measuring continuous, high-resolution stem water potentials. If applicable to forest trees, such sensors hold the potential to significantly enhance our understanding of tree water relations.

We evaluated these sensors in a temperate, diffuse-porous tree species (*Carpinus betulus*) over a growing season marked by dry-down periods and heat. Concurrent measurements of branch water potential, sap flow, and environmental factors (air temperature, vapor pressure deficit, and soil water content) were conducted. Midday stem water potentials of *C. betulus* reached minimum values of -3.39 ± 0.10 MPa and exhibited pronounced seasonal fluctuations, mirroring changes in environmental conditions and sap flow.

Comparison of stem water potentials with Scholander-type measurements revealed a very good correlation with predawn ($R^2 = 0.98$) and a general agreement with midday measurements ($R^2 = 0.71$). Diurnal variations in stem water potentials and sap flow exhibited a hysteresis, consistent with other plant parameters. In this first assessment, the agreement with Scholander-type measurements, sap flow, and environmental parameters suggests the tested water potential sensors yield reliable data. If applicable to other tree species, including conifers, these sensors could significantly advance our understanding of tree water relations and their role in forest drought responses.

Introduction

Plant water potential is an integrative and valuable parameter for assessing plant water stress, plant hydraulic strategies or plant drought resistance and resilience (Larcher, 1994; Steppe, 2018; Torres-Ruiz et al., 2024). Plant water relations are tightly linked to carbon assimilation and thus, a decline in plant water potentials will have a cascading effect on plant growth and production (Brodribb, 2009; McDowell, 2011; Torres-Ruiz et al., 2024). Under severe drought, plant water potential can drop below species-specific thresholds, triggering xylem cavitation and threatening plant survival (Choat et al., 2018; Schuldt et al., 2020). Currently, xylem failure under severe drought is thought to be the main cause for tree mortality (Choat et al., 2018; Mantova et al., 2022).

Up to date, the majority of plant water potentials are still measured using the Scholander pressure chamber (Scholander et al., 1965). While this method is well established and provides a robust way of assessing plant water potentials, measurements are time- and labor consuming (Steppe, 2018), destructive, sensitive to user errors (Rodriguez-Dominguez et al., 2022) and most importantly, do not provide the needed continuous data. For example, Guo et al. (2019) demonstrated a highly dynamic hydraulic behavior in the shrub *Larrea tridentata* with continuous water potential measurements, spanning from extreme anisohydric to partial isohydric in the course of only one growing season. Similarly, *Quercus suber* trees shifted their hydraulic behavior not only from wet to dry seasons, but also in response to species competition (Haberstroh et al., 2022a). While high frequency measurements (or the installation of expensive, high maintenance sensors, such as stem psychrometers) are in general viable for smaller vegetation (e.g. Guo et al., 2019), frequent measurements on tall forest trees are more challenging (Steppe, 2018), as either canopy access towers (e.g. Haberstroh et al., 2022b) or professional tree climbers are required to reach the tree crown for accurate measurements (e.g. Kinzinger et al., 2024).

Posted on 26 Aug 2024 — The copyright holder is the author/funder. All rights reserved. No reuse without permission. — https://doi.org/10.22541/au.172471102.26164569/v1 — This is a preprint and has not been peer-reviewed. Data may be preliminary.

Continuous, sensor-based plant water potential measurements under field conditions may advance our knowledge on rapid tree responses to extreme climatic events and can inform about short- and long-term dynamics in tree water relations and ecohydrological processes. In recent years, sensors based on microtensiometers were developed, mainly for agricultural purposes, such as irrigation management. Microtensiometer measurements in important agricultural woody species, such as apple trees (e.g. Gonzalez et al., 2022), grapevine or almond (Lasko et al., 2022), indicated a general agreement with traditional Scholander-type pressure chamber measurements.

Our main objectives were to test and validate sensors for continuous stem water potential measurements in the xylem of a diffuse-porous tree species and to determine their applicability in ecophysiological and ecohydrological research by comparing stem water potential measurements with traditional Scholander pressure chamber measurements, investigating seasonal environmental drivers of stem water potentials and relationship with sap flow. To test the sensors, we chose the deciduous broadleaf, diffuse porous hornbeam (*Carpinus betulus*) without notable resin production.

Material and Methods

Field site and tree species

To explicitly test stem water potential sensors of FloraPulse (Davis, CA, USA), we selected three hornbeam (*C. betulus*) trees at the Hartheim (Germany, 7.59814degE, 47.93391degN, 201 m a.s.l.) forest research site, an ICOS ecosystem site (DE-Har) operated by the University of Freiburg (Haberstroh et al., 2022b). The site is located on the alluvial plain of the Upper Rhine with a ground water table at 7m below the surface. For the period of 1991-2020 the field site's climate was characterized by an average air temperature of 11.0 degC and average annual precipitation of 640 mm. The forest research site was formerly dominated by *Pinus sylvestris* , however recent drought and heat events in combination with unfavorable site conditions (low groundwater table, shallow, sandy soils) initiated a vegetation shift towards broadleaved understory trees. One of the dominant understory species is *C. betulus* , which was more resistant during past drought events compared to *P. sylvestris* (Haberstroh et al., 2022b). The three chosen trees had a height of 10.0 – 10.5 m, a diameter at breast height of 16.0 – 18.7 cm and were growing in close vicinity to a 30 m canopy access tower to allow accessibility of the tree crowns for branch water potential measurements.

Meteorological measurements

Air temperature (T_{air}), relative humidity and vapour pressure deficit (VPD) were measured on site 2 m above ground in the forest canopy at with an actively ventilated psychrometer. Precipitation was measured above canopy (18 m) with an Ombrometer Model 5.4031 (Adolf Thies, Germany). Volumetric soil water content (VWC) was measured in two profiles and three depths (0.05, 0.10, 0.20 m, 0.50 and 1.00 m using CS655 soil moisture and temperature sensors, Campbell Scientific Logan, UT, USA). VWC values were averaged over the first three depths (0.05 – 0.20 m) and both profiles to describe a general trend of VWC in the topsoil.

Installation and operation of stem water potential sensors

Stem water potential sensors (microtensiometers, piezoresistive pressure transducer) with a size of 5 x 5 mm held in a cylindrical probe (8 mm diameter) were installed in May 2023 (cf. Lasko et al., 2022; Pagay, 2022). In detail, we installed the provided sleeve (14 mm outer diameter, 9 mm inner diameter) in the stem and ensured the xylem tissue was reached. Stem material within the sleeve was drilled to a depth of showed a bright white color, which was identified as active xylem tissue. Afterwards, the sleeve was filled with the provided mating compound (fine clay paste, Lasko et al., 2022) provided by FloraPulse before the sensor (8 mm cylindrical probe) was carefully inserted and tightened with a spring and cap. To avoid water infiltration, the sleeve and sleeve hole were covered with silicone grease (Fig. S1). Installation occurred ~1 m above the ground and sensors were shielded with reflective aluminum foil to avoid thermal influences of radiation. No further maintenance was required until November 2023, when sensors were de-installed. Stem water potential (Ψ_{Stem}) data was collected every 20 min on a Campbell CR1000 logger (Campbell Scientific, UT, USA). Predawn water potential (Ψ_{PD}) was calculated by averaging the measured values two hours

Posted on 26 Aug 2024 — The copyright holder is the author/funder. All rights reserved. No reuse without permission. — https://doi.org/10.22541/au.172471102.26164569/v1 — This is a preprint and has not been peer-reviewed. Data may be preliminary.

before sunrise. Midday water potential (Ψ_{MD}) was calculated by averaging values two hours after solar noon (CEST).

Scholander pressure chamber measurements

Scholander-type pressure chamber (1505D, PMS Instrument, USA) measurements (Scholander et al., 1965) were conducted predawn and midday over the course of the growing season from May to September 2023 at six days on branchlets of *C. betulus* (Ψ_{Branch}). Predawn water potential was measured between 4 and 6 am (CEST), but always before sunrise. Midday measurements were conducted between 1 and 3 pm (CEST) on sunlit branchlets of *C. betulus* approx. 8-10 m aboveground on sunny days. On September, 7th, Scholander type measurements were conducted every 1-2 hours from 6 am to 10 pm (CEST) to compare results with Ψ_{Stem}.

Sap flow measurements

In May, sap flow sensors (SFM1, ICT International, Armidale, Australia) were installed on the selected *C. betulus* trees at ~ 1.20 m height in close proximity to stem water potential sensors. Sensors consisted of three 35 mm stainless-steel needles, which were installed in the xylem to measure sap flow at 12.5 mm and 27.5 mm depth from the cambium. The needle placed in the middle served as heating element. Heat pulses (30 J) were generated every 20 minutes and data stored on internal loggers. Sap flux density (J_{s}) was calculated with the Heat Ratio Method (HRM, Marshall, 1958; Burgess et al., 2001) and averaged for both measured xylem depths. In nights with zero sap flow between May and November (defined as photosynthetically active photon flux density < 5 µmol m^{-2} s^{-1}, VPD < 0.05 kPa, $T_{\mathrm{air}} > 0$°C, RH > 95%), we corrected sap flow for offsets from the baseline (defined as zero sap flow).

Statistical analysis

For the comparison of Ψ_{Stem} and Ψ_{Branch}, we calculated a regression (linear mixed effects model) using the function *lme* in the R package *nlme* (Pinheiro et al., 2023). For the relationship of Ψ_{MD} calculated from Ψ_{Stem} we applied linear mixed effect models with T_{air} and VPD as predictors, respectively. Midday data were square-root transformed to comply with model assumptions. No clear relationship of Ψ_{PD} calculated from Ψ_{Stem} and T_{air} or VPD was found. The relationship between Ψ_{Stem} (predawn and midday) and VWC was best described by asymptotic regressions with the function*nlme* (Pinheiro et al., 2023). In all mixed effect models, tree identity was treated as random effect. To compare diurnal values of Ψ_{Stem} and Ψ_{Branch}, we calculated linear regressions (*lm*) for each tree separately. Depending on the tree individual, a lag between Ψ_{Stem} and Ψ_{Branch}, ranging from 100 to 220 minutes, determined by the best R^2 of the regressions. Model assumptions of linear mixed effect models (normal distribution of residuals) were tested with the Shapiro-Wilk test (*shapiro.test* in package *stats* , R Core Team, 2022). Conditional and marginal R^2 were obtained using the function *r.squared.GLMM* available in the R package *MuMIn* (Bartoń, 2022) for linear mixed effect models and with the function*R2M* in the package *nlraa* (Miguez, 2023) for non-linear mixed effect models. All statistical analysis was conducted with the open-source software R (version, 4.2.1, R Core Team, 2022).

Results

Meteorological conditions

2023 was characterized by a wet and moderately warm spring (Mar – May +0.13 K warmer than 1991-2020). This was followed by a summer (Jun – Aug) with much higher T_{air} (+1.13 K) and declining VWC from May onwards (Fig. 1). Two distinct periods with high T_{air} were identified on July 9th(T_{max}: 36.0°C) and on August 19th 2023 (T_{max}: 36.2°C), where daily maximum VPD ($\mathrm{VPD}_{\mathrm{max}}$) increased to values > 4 kPa (Fig. 1A). A steep decline of VWC from ~27% to < 10% occurred from mid-May to mid-June, where almost no precipitation was recorded (Fig. 1B). Despite frequent summer precipitation in July, VWC did not recover until November 2023. An analysis of meteorological conditions for the whole year showed that 2023 was the warmest year (12.3°C, +1.3 K) at the field site since climate records in 1978, while precipitation (606 mm, -34 mm) was close to the long-term average.

Posted on 26 Aug 2024 — The copyright holder is the author/funder. All rights reserved. No reuse without permission. — https://doi.org/10.22541/au.172471102.26164569/v1 — This is a preprint and has not been peer-reviewed. Data may be preliminary.

Seasonal development of stem water potential and sap flow

Environmental conditions (Fig. 1) were reflected in water potentials and sap flow of *C. betulus* (Fig. 2). From May to July, Ψ_{Stem} decreased from values close to 0 MPa to -1.03 ± 0.16 MPa (Ψ_{PD}, Fig. 2A) and -2.37 ± 0.21 MPa (Ψ_{MD}, Fig. 2B). Afterwards, Ψ_{Stem}developed more dynamically due to more frequent precipitation events (Fig. 1B) until a distinct dry-down period with high T_{air} was observed in mid-August, leading to minimum Ψ_{PD} (-1.59 ± 0.13 MPa) and Ψ_{MD} (-3.39 ± 0.10 MPa). For predawn conditions, continuous Ψ_{Stem} and destructive Ψ_{Branch} measurements showed a good agreement in dynamics and absolute values with the expectation of late-August 2023, where Ψ_{Branch} dropped to -2.27 ± 0.19 MPa compared to -1.49 +- 0.14 MPa of Ψ_{Stem} (Fig. 2A). Under midday conditions, Ψ_{Branch} also resembled the dynamics of Ψ_{Stem}, however absolute values were mostly lower, particularly visible in September 2023 (with one exception in mid-August 2023, where Ψ_{Stem} was lower compared to Ψ_{Branch} (Fig. 2B)). Both, Ψ_{PD} and Ψ_{MD} extracted from Ψ_{Stem} recovered to values close to 0 MPa during the rewetting period in early October.

Daily sap flux density (J_s) of *C. betulus* increased in spring 2023 in accordance with rising $T_{\text{air}}$and VPD_{max} (Fig. 1A) to max. values of 235.7 ± 25.0 $\text{cm}^3\ \text{cm}^{-2}\ \text{day}^{-1}$. With declining VWC, J_s decreased over the first half of summer, similarly to Ψ_{Stem}, until July. Afterwards, dynamics in J_s mostly resembled dynamics in Ψ_{Stem}, e.g. also with a distinct second dry-down period in late-August and J_s close to 0 $\text{cm}^3\ \text{cm}^{-2}\text{day}^{-1}$ (Fig. 2C). After leaf senescence starting in mid-October, J_s ceased in early November, in agreement with high Ψ_{Stem}.

Comparison of stem and branch water potential

The agreement between Ψ_{Branch} and $\Psi_{\text{Stem}}$was reasonable, however differed between Ψ_{PD} and Ψ_{MD} (Fig. 3, Fig. S2-S6). For Ψ_{PD}, the relationship of both parameters was highly significant ($p<0.001$, $R^2_c = 0.98$). Ψ_{Branch} was slightly lower than Ψ_{Stem}, which was especially evident in August 2023 (Fig. 2A), leading to a slope of the regression in Fig. 3A of 1.49±0.05 MPa MPa^{-1}. Interestingly, the largest discrepancy between Ψ_{Branch} and Ψ_{Stem} was measured when VPD values did not drop below 0.19 kPa in the night (August 23rd), which led to nocturnal sap flow of *C. betulus* at the time of predawn measurements of Ψ_{Branch}(Fig. S5).

The relationship of Ψ_{Branch} and Ψ_{Stem}during midday was more variable (Fig. 3B), but highly significant ($p<0.001$, $R^2_c = 0.71$). Interestingly, the slope of the regression was below 1 (0.38±0.06 MPa MPa^{-1}). Potentially, this was due to missing Ψ_{Branch}measurements above -1.50 MPa and missing measurements on cloudy days. Thus, the relationship of Ψ_{Branch} and Ψ_{Stem} presented here might only be reliable for the given measurement range on sunny days and might need validation for higher Ψ_{MD} values.

Diurnal courses were measured at the end of the study period, when predawn potentials were high, and indicated a very good agreement between Ψ_{Branch} and Ψ_{Stem} ($R^2 = 0.81 - 0.86$), albeit with three specific differences: 1) Ψ_{Branch} was significantly lower and showed a stronger diurnal amplitude than Ψ_{Stem} (Fig. 4A,C,E), 2) there was a strong lag between Ψ_{Branch} and Ψ_{Stem}ranging from 100 to 220 minutes, (3) and the relationship of Ψ_{Branch} and Ψ_{Stem} different between trees (Fig. 4B,D,F). As Ψ_{Branch} and Ψ_{Stem} were measured on different parts of the trees and trees had different positions in the forest canopy regarding environmental conditions, such as light, we further evaluated Ψ_{Stem} with data of sap flow sensors installed in the stem and environmental conditions.

Diurnal courses of sap flow and stem water potential

As expected, J_s and Ψ_{Stem} showed opposing diurnal courses for all measured trees, and agreed in dynamics (Fig. 5). While J_s increased strongly between 7 am and 3 pm (CEST, on average), Ψ_{Stem} decreased simultaneously. Between 3 pm and 7 am (CEST, on average), this pattern was reversed. However, the relationship of the two parameters was different in the two time periods (Fig. 5A,C,E), indicating a hysteresis (Fig. 5B,D,F). With increasing J_s, Ψ_{Stem} simultaneously decreased, however maximum J_s was reached, 100-120 min before minimum Ψ_{Stem} occurred. After maximum J_s was reached, J_s decreased quickly and approached values of $< 0.5\ \text{cm}^3\ \text{cm}^{-2}$ already in the early evening. Yet, Ψ_{Stem} recovered significantly slower, only approaching initial values after midnight (Fig. 5A,C,E).

Posted on 26 Aug 2024 — The copyright holder is the author/funder. All rights reserved. No reuse without permission. — https://doi.org/10.22541/au.172471102.26164569/v1 — This is a preprint and has not been peer-reviewed. Data may be preliminary.

Relationship of stem water potential with environmental parameters

Besides comparing Ψ_{Stem} with Ψ_{Branch} and J_s, we evaluated the relationship of Ψ_{Stem} with the concurrently measured environmental parameters T_{air}, $\mathrm{VPD}_{\mathrm{max}}$ and VWC (Fig. 6). For Ψ_{PD} there was a weak tendency of decreasing values with rising T_{air} and $\mathrm{VPD}_{\mathrm{max}}$ (Fig. 6A,C). *C. betulus* mainly responded to soil drying (VWC, $R^2 = 0.59$) with a drop of Ψ_{PD}, especially when VWC declined below ˜ 8% (Fig. 6E). Ψ_{MD} of *C. betulus* decreased simultaneously with increasing $\mathrm{VPD}_{\mathrm{max}}$($R^2{}_c = 0.59$, $p<0.001$), T_{air}($R^2{}_c = 0.48.$, $p<0.001$) and decreasing VWC ($R^2{}_c = 0.74$) (Fig. 6B,D,F). Thus, plants reacted strongly to a combination of drier and hotter conditions.

Discussion

In general, stem water potentials obtained for *C. betulus* agreed well with traditional Scholander pressure chamber measurements (Ψ_{Branch}), with minor deviations), sap flow dynamics and environmental conditions. We identified three patterns between Ψ_{Stem} and Ψ_{Branch} measurements that require further discussion: 1) significant lower seasonal Ψ_{PD} ($\Delta\ \Psi_{\mathrm{PD}} = 0.6 - 1$ MPa, $p < 0.001$, linear mixed effect model) values in the branch compared to the stem during dry periods, 2) the difference between $\Psi_{\mathrm{Stem}}$and Ψ_{Branch} in seasonal (Ψ_{MD}) and diurnal measurements in absolute values, variability and magnitude, and 3) the (tree-individual) hysteresis of Ψ_{Stem} compared to J_s and Ψ_{Branch}.

Potential predawn disequilibrium has to be considered

In theory, plant water potential equilibrates with soil water potential during night, when water reserves are replenished (Hinckley et al., 1978; Richter, 1997). Thus, during predawn conditions, Ψ_{Stem} and Ψ_{Branch} should be equal or at least very similar, as was the case during most of the study period (Fig. 2A, Fig. 4). However, during drier periods, predawn Ψ_{Branch} was 0.6 – 1.0 MPa lower than Ψ_{Stem} (Fig. S5), which may indicate an incomplete refilling of tree water reserves. Such behaviour has also been observed under non-drought conditions (Donovan et al., 2001; 2003), and has been attributed to the occurrence of nocturnal transpiration (Donovan et al., 2003; Kavanagh et al., 2007; Kangur et al., 2021) and high nocturnal VPD (Kangur et al., 2017). Our data suggests that predawn disequilibrium actually occurred during nights of high VPD and led to the observed discrepancy of Ψ_{Stem} and Ψ_{Branch} under dry conditions. Thus, Ψ_{Branch} should be measured over a large range of predawn conditions (including severe drought) to verify Ψ_{Stem} measurements and to account for predawn disequilibrium.

$\Psi_{\Sigma\tau\epsilon\mu}$ *ις βυφφερεδ ςομπαρεδ το* $\Psi_{B\rho\alpha\nu\varsigma\eta}$

During high sap flow, a significant water potential gradient is building up within the plant during the day (e.g. Larcher, 1994). As we measured Ψ_{Stem} at ˜1 m and Ψ_{Branch}at ˜8-10 m height, differences in absolute values, magnitude and variability of Ψ are to be expected during the day. Ψ in the stem are buffered compared to Ψ in terminal branches, express higher Ψ and a lower diurnal variability (Jarvis, 1976; Larcher, 1994; Scholz et al., 2007; Nikinmaa et al., 2014). Ψ_{Branch} and J_s-measurements in the tree crown are highly variable and reflect the diverse, often fast changing microclimatic conditions, such as light levels (e.g. Burgess and Dawson, 2008), while Ψ_{Stem} is, similar to J_s at the stem base, an integrative signal of the tree's response, comprising the response of all branches and leaves in the tree crown. The data presented for Ψ_{MD} (Fig. 2B) and the diurnal course on the September 7th (Fig. 4) nicely illustrate this difference between Ψ measurements on different positions within the soil-plant-atmosphere continuum and tree crown, and thus it is reasonable to assume that the data presented here are valid with two minor restrictions: 1) The regression of Ψ_{Stem} and Ψ_{Branch} for midday conditions shown in Fig. 3B might only be valid for sunny days, as we did not measure Ψ_{Branch} on cloudy days. 2) On August 23rd, Ψ_{Stem} was lower than Ψ_{Branch} (Fig. S5), which might question the accuracy of the stem water potential sensor close to its operating limit given by the manufacturer (-3.5 MPa). However, Ψ_{Stem} and J_s clearly illustrate the same diurnal patterns (Fig. S5). Thus, it seems possible that the measured leaves were not representative for the total tree water potential under such dry conditions. On one hand, C. *betulus* suffered from drought-induced leaf senescence and crown cover reduction already in August, a common feature of *C. betulus* in dry periods (Richter et al., 2022; Leuschner et al., 2024). On the other hand, vulnerability segmentation under drought is increasingly discussed (Tyree and Ewers, 1991;

Posted on 26 Aug 2024 — The copyright holder is the author/funder. All rights reserved. No reuse without permission. — https://doi.org/10.22541/au.172471102.26164569/v1 — This is a preprint and has not been peer-reviewed. Data may be preliminary.

Charrier et al., 2016; Wilkening et al., 2023), where different plant organs do show different vulnerabilities to cavitation. However, to test different vulnerabilities of branches and stems of *C. betulus* to cavitation, more specified experiments are required. Although measurement errors of stem water potential sensors cannot be excluded, the match of diurnal Ψ_{Stem} and $\mathrm{J_s}$dynamics for all measured trees (Fig. S2 – Fig. S5) is promising.

Τηϵ ηψστερϵσις ανδ λαγ οφ $\Psi_{\Sigma\tau\epsilon\mu}$ *ωιτη* Θ_{ς} *ανδ* $\Psi_{B\rho\alpha\nu\varsigma\eta}$ *ραισϵ τηϵ χυϵστιον οφ στϵμ ςαπαςιτανςϵ*

The occurrence of hysteresis in plant water relations is well known and has been observed for water fluxes in stem and needles/leaves (e.g. Larcher, 1994), xylem diameter variations and sap flow (e.g. Sevanto et al., 2008) and stem water potential and sap flow (e.g. Stöhr and Lösch, 2004). The latter two have been connected to usage of stored water in stem and bark, which can be exchanged with and released into the transpiration stream (Wullschleger et al., 1998; Zweifel et al., 2001; Scholz et al., 2011). This capacitive discharge can buffer daily variations in xylem tension, preventing embolism and hydraulic dysfunction (Scholz et al., 2011). For example, higher stem capacitance led to less negative leaf Ψ_{MD} in tropical species (Scholz et al., 2007), and allowed *Pinus halepensis* to maintain a sufficient hydraulic safety margin during the dry season (Preisler et al., 2021). Thus, it is likely that the hysteresis of Ψ_{Stem} and $\mathrm{J_s}$ in *C. betulus* was caused by the release of stored water to buffer fluctuations in xylem tension. Likewise, the lag of Ψ_{Stem} and Ψ_{Branch} during our diurnal measurements (Fig. 4) was potentially caused by similar mechanisms. As measurements were conducted in a period of high Ψ_{PD}, stem water reserves were most likely filled, leading to only minor variations in xylem tension. Low Ψ_{Branch} at the same time point towards an increasing physiological activity, also evident from increasing $\mathrm{J_s}$, after recovery rainfall at the beginning of September. Especially for Tree 3 (Fig. 4E), the question arises, if Ψ_{Stem} was representative for Ψ_{Branch} on this day, as only a minor diurnal variation (˜0.20 MPa) in Ψ_{Stem} was observed, although Ψ_{Branch} dropped to values $<$ -2.0 MPa. Either Ψ_{Stem} measurements were erroneous, or there is the possibility of within species tree individual capacitance differences, similar to between species differences in capacitance (Scholz et al., 2007; Scholz et al., 2011). In conclusion, the measurement day in September was not ideal and the diurnal variation of Ψ_{Stem} and Ψ_{Branch} should also be measured during dry periods to better establish a relationship between the two parameters over a larger range of environmental conditions. Additionally, stem diameter variations and tree water deficit (TWD) (Zweifel et al., 2016), calculated via dendrometers, may be a promising approach to validate Ψ_{Stem} (cf. Dietrich et al., 2018), as xylem tension and stem diameter changes are closely related (Irvine and Grace, 1997).

Stem water potentials correlate well with environmental conditions

The obtained Ψ_{PD} and Ψ_{MD} from Ψ_{Stem} correlated well with dominant environmental conditions, illustrating their general applicability. The regressions shown in Fig. 6D and F mirror the relationship of sap flow and $\mathrm{VPD_{max}}$ / VWC under edaphic and atmospheric drought (e.g. Sanchez-Costa et al., 2015; Haberstroh et al., 2022a), as well as the relation of maximum TWD and soil moisture (Brinkmann et al., 2016). TWD, similarly to Ψ_{MD}, showed a sharp increase after a threshold of VWC was reached, indicating increased drought stress for trees. This relationship points towards a close relationship of Ψ_{Stem} and TWD, also indicated by TWD modelling, which works best, when both, VPD and soil water potential, are included (Zweifel et al., 2006).

Conclusion

Stem water potentials obtained continuously with microtensiometers offer a high potential for ecophysiological and ecohydrological stress research, if applicable in other important tree species. In combination with other ecophysiological measures, such as sap flow or tree water deficits, tree stress can be detected and investigated dynamically. Continuous stem water potential data further have the potential to improve modelling approaches of tree drought response and mortality events (Steppe, 2018; Hartmann et al., 2018) and allow for a better investigation of stem capacitance, as data on capacitance and water potential, measured on the same location are scarce, but pivotal for capacitance studies (Scholz et al., 2011). Beside these fundamental findings on processes, the effort to obtain data changes drastically, as continuous data sets can be collected without time- and labor consuming Scholander pressure chamber measurements.

The data presented here is promising, although stem water potential sensors need to be rigorously evaluated

Posted on 26 Aug 2024 — The copyright holder is the author/funder. All rights reserved. No reuse without permission. — https://doi.org/10.22541/au.172471102.26164569/v1 — This is a preprint and has not been peer-reviewed. Data may be preliminary.

for every species. In particular, the relationship of Ψ_{Stem} and Ψ_{Branch} data requires further assessments in different contexts. Ψ_{Stem} can provide a more integrative measure of stress that includes the response to environmental factors of an entire forest canopy, while Ψ_{Branch} or Ψ_{Leaf} are additionally dependent on the diverse, fast changing environmental conditions in the tree crown, representing a specific part of the canopy. In conclusion, continuous stem water potential data have a high potential in advancing our knowledge about tree and forest drought responses.

Conflict of Interest

None declared.

Data Availability

The data that support the findings of this study are available from the corresponding author upon reasonable request.

References

Bartoń, K. (2022). MuMIn: Multi-Model Inference. R package version 1.47.1, https://CRAN.R-project.org/package=MuMIn.

Brinkmann, N., Eugster, W., Zweifel, R., Buchmann, N., & Kahmen, A. (2016). Temperate tree species show identical response in tree water deficit but different sensitivities in sap flow to summer soil drying. Tree Physiology, 36, 1508-1519. doi:10.1093/treephys/tpw062

Brodribb, T.K. (2009). Xylem hydraulic physiology: The functional backbone of terrestrial plant productivity. Plant Science, 177, 245-251. doi:10.1016/j.plantsci.2009.06.001

Burgess, S.S.O, Adams, M.A., Turner, N.C., Beverly, C.R., Ong, C.K., Khan, A.A.H., et al. (2001). An improved heat pulse method to measure low and reverse rates of sap flow in woody plants. Tree Physiology, 21, 589-598. doi:10.1093/treephys/21.9.589

Burgess, S.S.O, & Dawson, T.E. (2008). Using branch and basal trunk sap flow measurements to estimate whole-plant water capacitance: a caution. Plant Soil, 305, 5-13. doi:10.1007/s11104-007-9378-2

Charrier, G., Torres-Ruiz, J.M., Badel, E., Burlett, R., Choat, B., Cochard, H., et al. (2016). Evidence for hydraulic vulnerability segmentation and lack of xylem refilling under tension. Plant Physiology, 172, 1657-1668. doi:10.1104/pp.16.01079

Choat, B., Brodribb, T.J., Brodersen, C.R., Duursma, R.A., López, R., & Medlyn, B. (2018). Triggers of mortality under drought. Nature, 558, 531-539. doi:10.1038/s41586-018-0240-x

Dietrich, L., Zweifel, R., & Kahmen, A. (2018). Daily stem diameter variations can predict the canopy water status of mature temperate trees. Tree Physiology, 38, 941-952. doi:10.1093/treephys/tpy023

Donovan, L.A., Linton, M.J., & Richards, J.H. (2001). Predawn plant water potential does not necessarily equilibrate with soil water potential under well-watered conditions. Oecologia, 129, 328-335. doi:10.1007/s004420100738

Donovan, L.A., Richards, J.H., & Linton, M.J. (2003). Magnitude and mechanisms of disequilibrium between predawn plant and soil water potentials. Ecology, 84, 463-470. doi:10.1890/0012-9658(2003)084[0463:MAMODB]2.0.CO;2

González, L., Huber, A., Gao, R., Cheng, L., Stroock, A.D., Lasko, A.N., & Robinson, T.L. (2022). Using micro-tensiometers to manage water stress to maximize fruit size of apple orchards. Acta Horticulturae, 1373, 113-120. doi:10.17660/ActaHortic.2023.1373.16

Guo, J.S., Hultine, K.R., Koch, G.W., Kropp, H., & Ogle, K. (2019). Temporal shifts in iso/anisohydry revealed from daily observations of plant water potential in a dominant desert shrub. New Phytologist, 225, 713-726. doi:10.1111/nph.16196

Posted on 26 Aug 2024 — The copyright holder is the author/funder. All rights reserved. No reuse without permission. — https://doi.org/10.22541/au.172471102.26164569/v1 — This is a preprint and has not been peer-reviewed. Data may be preliminary.

Hinckley, T.M., Lassoie, J.P., & Running, S.W. (1978). Temporal and spatial variations in the water status of forest trees. Forest Science, 24, a0001-z0001. doi:10.1093/forestscience/24.s1.a0001

Haberstroh, S., Lobo-do-Vale, R., Caldeira, M., Dubbert, M., Cuntz, M., & Werner, C. (2022a) Plant invasion modifies isohydricity of Mediterranean tree species. Functional Ecology, 36, 2384-2398. doi:10.1111/1365-2435.14126

Haberstroh, S., Werner, C., Grün, M., Kreuzwieser, J., Seifert, T., Schindler, D., & Christen, A. (2022b). Central European 2018 hot drought shifts scots pine forest to its tipping point. Plant Biology, 24, 1186-1197. doi:10.1111/plb.13455

Hartmann, H., Moura, C.F., Anderegg, W.R.L., Ruehr, N.K., Salmon, Y., Allen, C.D., et al. (2018). Research frontiers for improving our understanding of drought-induced tree and forest mortality. New Phytologist, 218, 15-28. doi:10.1111/nph.15048

Irvine, J., & Grace, J. (1997). Continuous measurements of water tensions in the xylem of trees based on the elastic properties of wood. Planta, 202, 455-461. doi:10.1007/s004250050149

Jarvis, P.G. (1976). The interpretation of the variations in leaf water potential and stomatal conductance found in canopies in the field. Philosophical Transactions of the Royal Society of London. Series B, Biological Sciences, 273, 593-610. doi:10.1098/rstb-1976.0035

Kangur, O., Kupper, P., & Sellin, A. (2017). Predawn disequilibrium between soil and plant water potentials in light of climate trends predicted for northern Europe. Regional Environmental Change, 17, 2159-2168. doi:10.1007/s10113-017-1183-8

Kangur, O., Steppe, K., Schreel, J.D.M., von der Crone, J.S., & Sellin, A. (2021). Variation in nocturnal stomatal conductance and development of predawn disequilibrium between soil and leaf water potentials in nine temperate deciduous tree species. Functional Plant Biology, 48, 483-492. doi:10.1071/FP20091

Kavanagh, K.L., Pangle, R., & Schotzko, A.D. (2007). Nocturnal transpiration causing disequilibrium between soil and stem predawn water potential in mixed conifer forests of Idaho. Tree Physiology, 27, 621-629. doi:10.1093/treephys/27.4.621

Kinzinger, L., Mach, J., Haberstroh, S., Schindler, Z., Frey, J., Dubbert, M., et al. (2024). Interaction between beech and spruce trees in temperate forests affects water use, root water uptake pattern and canopy structure. Tree Physiology, 44, tpad144. doi:10.1093/treephys/tpad144

Larcher, W. (1994). Ökophysiologie der Pflanzen (5th ed.). Stuttgart, Germany, Verlag Eugen Ulmer Stuttgart.

Lasko, A.M., Santiago, M., & Stroock, A.D. (2022). Monitoring Stem water potential with an embedded microtensiometer to inform irrigation scheduling in fruit crops. Horticulturae, 8, 1207. doi:10.3390/horticulturae8121207

Leuschner, C., Fuchs, S., Wedde, P., Rüther, E., & Schuldt, B. (2024). A multi-criteria drought resistance assessment of temperate *Acer, Carpinus, Fraxinus, Quercus* , and *Tilia* species. Perspectives in Plant Ecology, 62, Evolution and Systematics, 125777. doi:10.1016/j.ppees.2023.125777

Mantova, M., Herbette, S., Cochard, H., & Torres-Ruiz, J.M. (2022). Hydraulic failure and tree mortality: from correlation to causation. Trends in Plant Science, 27, 335-345. doi:10.1016/j.tplants.2021.10.003

Marshall, D.C. (1958). Measurement of sap flow in conifers by heat transport. Plant Physiology, 33, 385-396. doi:10.1104/pp.33.6.385

McDowell, N.G. (2011). Mechanisms linking drought, hydraulics, carbon metabolism, and vegetation mortality. Plant Physiology, 155, 1051-1059. doi:10.1104/pp.110.170704

Posted on 26 Aug 2024 — The copyright holder is the author/funder. All rights reserved. No reuse without permission. — https://doi.org/10.22541/au.172471102.26164569/v1 — This is a preprint and has not been peer-reviewed. Data may be preliminary.

Miguez, F. (2023). nlraa: Nonlinear Regression for Agricultural Applications. R package version 1.9.3, https://CRAN.R-project.org/package=nlraa.

Nikinmaa, R., Sievänen, R., & Hölttä, T. (2014). Dynamics of leaf gas exchange, xylem and phloem transport, water potential and carbohydrate concentration in a realistic 3-D model tree crown. Annals of Botany, 114, 653-66. doi:10.1093/aob/mcu068

Pagay, V. (2022). Evaluating a novel microtensiometer for continuous trunk water potential measurements in field-grown irrigated grapevines. Irrigation Science, 40, 45-54. doi:10.1007/s00271-021-00758-8

Pinheiro, J., Bates, D., & R Core Team (2023). nlme: Linear and Nonlinear Mixed Effects Models. R package version 3.1-163, https://CRAN.R-project.org/package=nlme.

Preisler, Y., Holtta, T., Grunzweig, J.M., Oz, I., Tatarinov, F., Ruehr, N.K., et al. (2021). The importance of tree internal water storage under drought conditions. Tree Physiology, 42, 771-783. doi:10.1093/treephys/tpab144

R Core Team (2022). R: A language and environment for statistical computing. R Foundation for Statistical Computing, Vienna, Austria. https://www.R-project.org/.

Richter, H. (1997). Water relations in the field: some comments on the measurement of selected parameters. Journal of Experimental Botany, 48, 1-7. doi:10.1093/jxb/48.1.1

Richter, R., Ballasus, H., Engelmann, R.A., Zielhofer, C., Sanaei, A., & Wirth, C. (2022). Tree species matter for forest microclimate regulation during the drought year 2018: disentangling environmental drivers and biotic drivers. Scientific Reports, 12, 17559. doi:10.1038/s41598-022-22582-6

Rodriguez-Dominguez, C.M., Forner, A., Martorell, S., Choat, B., Lopez, R., Peters, J.M.R., et al. (2022). Leaf water potential measurements using the pressure chamber: Synthetic testing of assumptions towards best practices for precision and accuracy. Plant, Cell & Environment, 45, 2037-2061. doi:10.1111/pce.14330

Sanchez-Costa, E., Poyatos, R., & Sabate, S. (2015). Contrasting growth and water use strategies in four co-occurring Mediterranean tree species revealed by concurrent measurements of sap flow and stem diameter variations. *Agricultural and Forest Meteorology* , 207, 24-37. doi:10.1016/j.agrformet.2015.03.012

Scholander, P.F., Bradstreet, E.D., Hemmingsen, E.A., & Hammel, H.T. (1965). Sap pressure in vascular plant: negative hydrostatic pressure can be measured in plants. Science, 148, 339-346. doi:10.1126/science.148.3668.339

Scholz, F.G., Bucci, S.J., Goldstein, G., Meinzer, F.C., Franco, A.C., & Miralles-Wilhelm, F. (2007). Biophysical properties and functional significance of stem water storage tissues in Neotropical savanna trees. Plant, Cell & Environment, 30, 236-248. doi:10.1111/j.1365-3040.2006.01623.x

Scholz, F.G., Phillips, N.G., Bucci, S.J., Meinzer, F.C., & Goldstein, G. (2011). Hydraulic capacitance: biophysics and functional significance of internal water sources in relation to tree size. In: F.C. Meinzer, B. Lachenbruch, T.E. Dawson, eds. *Size- and age-related changes in tree structure and function.* Springer Science & Business Media.

Schuldt, B., Buras, A., Arend, M., Vitasse, Y., Beierkuhnlein, C., Damm, A., et al. (2020). A first assessment of the impact of the extreme 2018 summer drought on Central European forests. Basic and Applied Ecology, 45, 86-103. doi:10.1016/j.baae.2020.04.003

Sevanto, S., Nikinmaa, E., Rikkonen, A., Daley, M., Pettijohn, J.C., Mikkelsen, T.N., et al. (2008). Linking xylem diameter variation with sap flow measurements. Plant Soil, 305, 77-90. doi:10.1007/s11104-008-9566-8

Steppe, K., (2018). The potential of the tree water potential. Tree Physiology, 38, 937-940. doi:10.1093/treephys/tpy064

Posted on 26 Aug 2024 — The copyright holder is the author/funder. All rights reserved. No reuse without permission. — https://doi.org/10.22541/au.172471102.26164569/v1 — This is a preprint and has not been peer-reviewed. Data may be preliminary.

Torres-Ruiz, J.M., Cochard, H., Delzon, S., Boivin, T., Burlett, R., Cailleret, M., et al. (2024). Plant hydraulics at the heart of plant, crops and ecosystem functions in the face of climate change. New Phytologist, 241, 984-999. doi:10.1111/nph.19463

Tyree, M.T., & Ewers, F.W. (1991). The hydraulic architecture of trees and other woody plants. New Phytologist, 119, 345-360. doi:10.1111/j.1469-8137.1991.tb00035.x

Stohr, A., & Losch, R. (2004). Xylem sap flow and drought stress of*Fraxinus excelsior* sapling. Tree Physiology, 24, 169-180. doi:10.1093/treephys/24.2.169

Werner, C., Wallrabe, U., Christen, A., Comella, L., Dormann, C., Goritz, A., (2024). ECOSENSE - Multi-scale quantification and modelling of spatio-temporal dynamics of ecosystem processes by smart autonomous sensor networks. Research Ideas and Outcomes, 10, e129357. doi:10.3897/rio.10.e129357

Wilkening, J.V., Skelton, R.P., Feng, X., Dawson, T.E., & Thompson, S.E. (2023). Exploring within-plant hydraulic trait variation: A test of the vulnerability segmentation hypothesis. Plant, Cell & Environment, 46, 2726-2746. doi:10.1111/pce.14649

Wullschleger, S.D., Meinzer, F.C., & Vertessy, R.A. (1998). A review of whole-plant water use studies in trees. Tree Physiology, 18, 499-512. doi:10.1093/treephys/18.8-9.499

Zweifel, R., Item, H., & Hasler, R. (2001). Link between diurnal stem radius changes and tree water relations. Tree Physiology, 21, 869-877. doi:10.1093/treephys/21.12-13.869

Zweifel, R., Zimmermann, L., Zeugin, F., & Newberry, D.M. (2006). Intra-annual radial growth and water relations of trees: implications towards a growth mechanism. Journal of Experimental Botany, 57, 1445-1459. doi:10.1093/jxb/erj125

Zweifel, R., Haeni, M., Buchmann, N., & Eugster, W. (2016). Are trees able to grow in periods of stem shrinkage? New Phytologist, 211, 839-849. doi:10.1111/nph.13995

Figure Legends

Figure 1. Seasonal development of daily average air temperature (T_{air}) with maximum and minimum T_{air}, maximum vapour pressure deficit (VPD_{max}) (both A), volumetric soil water content (+- 1SE) and precipitation (both B) at the forest research site in Hartheim.

Figure 2. Predawn (A), midday (B) stem water potential (Ψ_{Stem}) and sap flux density (J_s) with 95% Confidence Interval from May to September 2023. In panels A and B, branch water potentials (Ψ_{Branch}) ± 1 SE are shown as triangles. Ψ_{Stem} measurements were conducted with FloraPulse stem water potential sensors. Ψ_{Branch} was measured with the Scholander Pressure Chamber. In September, logger failure caused a data loss of two weeks for Ψ_{Stem}.

Figure 3. Regression (linear mixed effect model) of stem water potential (Ψ_{Stem}) and branch water potential (Ψ_{Branch}) for predawn (A) and midday conditions (B) with conditional R^2.

Figure 4. Diurnal course of stem water potential (Ψ_{Stem}) and branch water potential (Ψ_{Branch}) on September 7th for all measured trees (A, C, E) and the regression between Ψ_{Stem} and Ψ_{Branch} with R^2 including a lag of 100-220 minutes (B, D, F). Note the different scales for Ψ_{Stem} and Ψ_{Branch}.

Figure 5. Average diurnal course of sap flux density (J_s) ± 1 SE and stem water potential (Ψ_{Stem}) ± 1 SE for all measured trees (A, C, E) and relationship of J_s ± 1 SE and Ψ_{Stem} ± 1 SE for all measured trees (B, D, F) between May and October 2023. Values after October were not considered due to leaf senescence.

Figure 6. Relationship of Ψ_{Stem} with air temperature (T_{air}) (A, B), maximum vapour pressure deficit (VPD_{max}) (C, D) and volumetric soil water content (VWC) (E, F) or predawn (A, C, E) and midday conditions (B, D, F). Values after October were not considered due to leaf senescence.

Posted on 26 Aug 2024 — The copyright holder is the author/funder. All rights reserved. No reuse without permission. — https://doi.org/10.22541/au.172471102.26164569/v1 — This is a preprint and has not been peer-reviewed. Data may be preliminary.

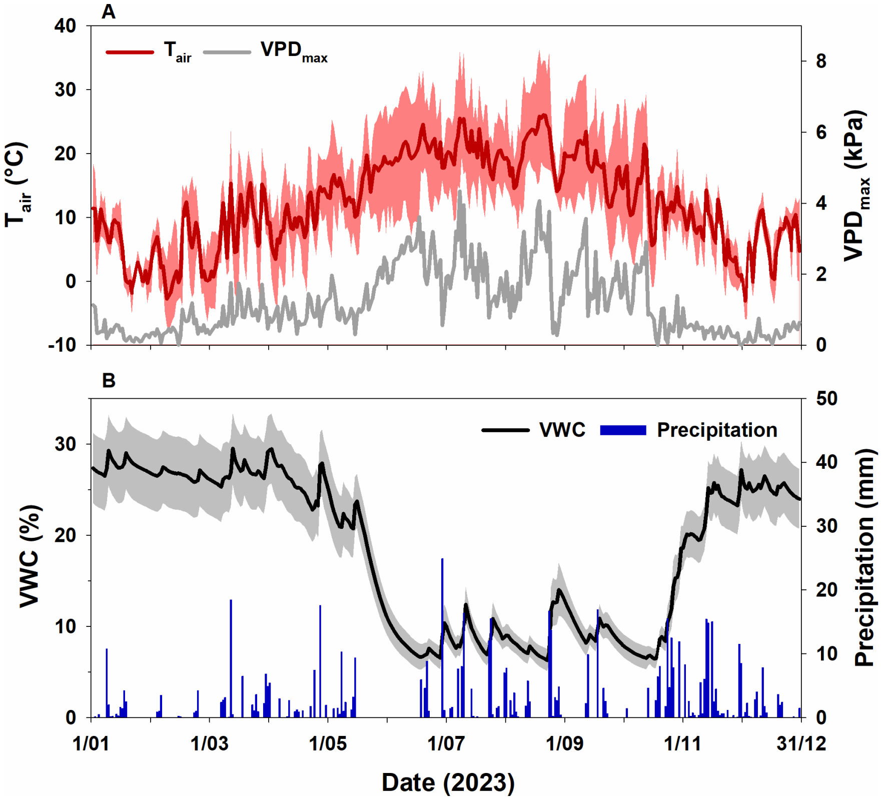

Posted on 26 Aug 2024 — The copyright holder is the author/funder. All rights reserved. No reuse without permission. — https://doi.org/10.22541/au.172471102.26164569/v1 — This is a preprint and has not been peer-reviewed. Data may be preliminary.

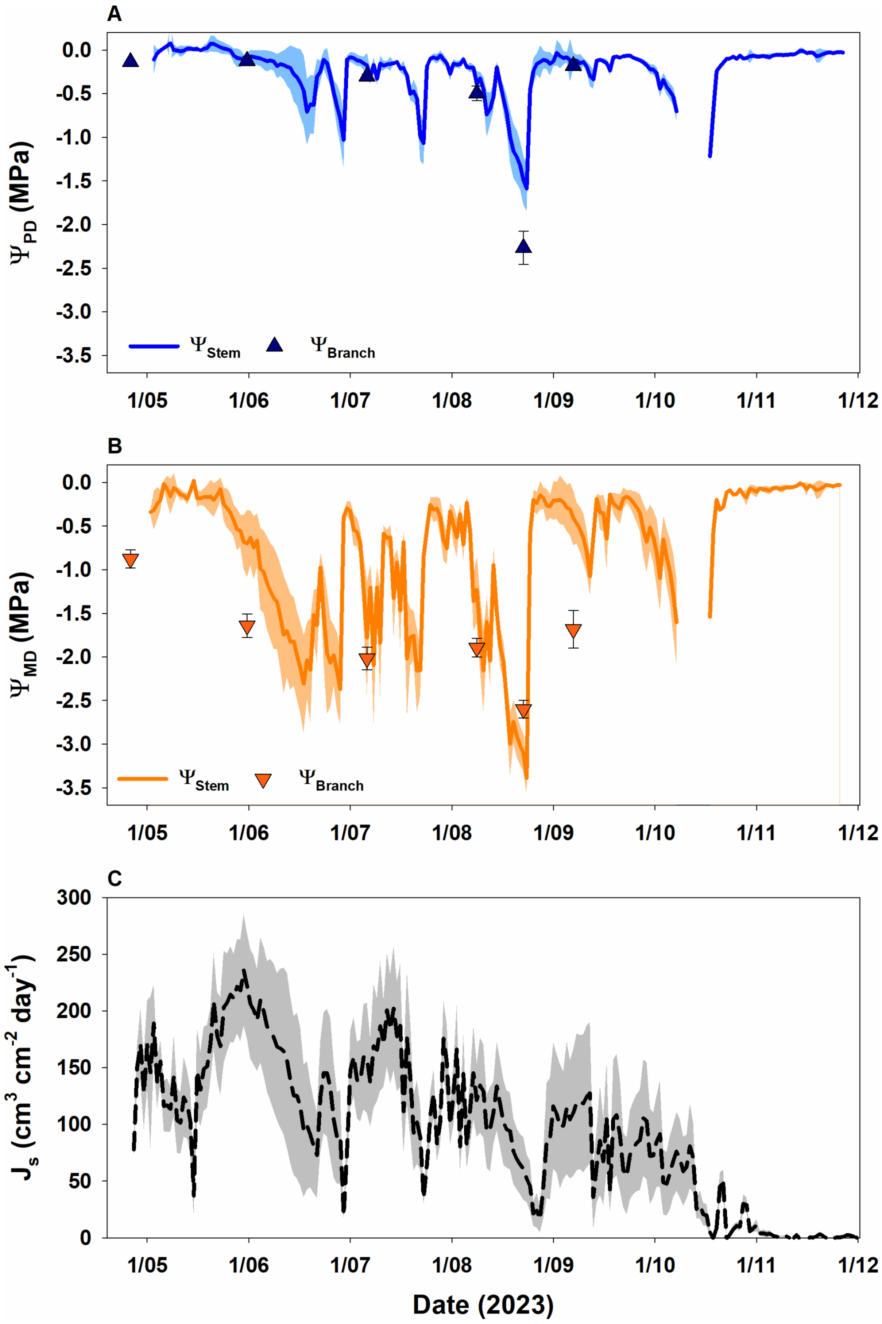

Posted on 26 Aug 2024 — The copyright holder is the author/funder. All rights reserved. No reuse without permission. — https://doi.org/10.22541/au.172471102.26164569/v1 — This is a preprint and has not been peer-reviewed. Data may be preliminary.

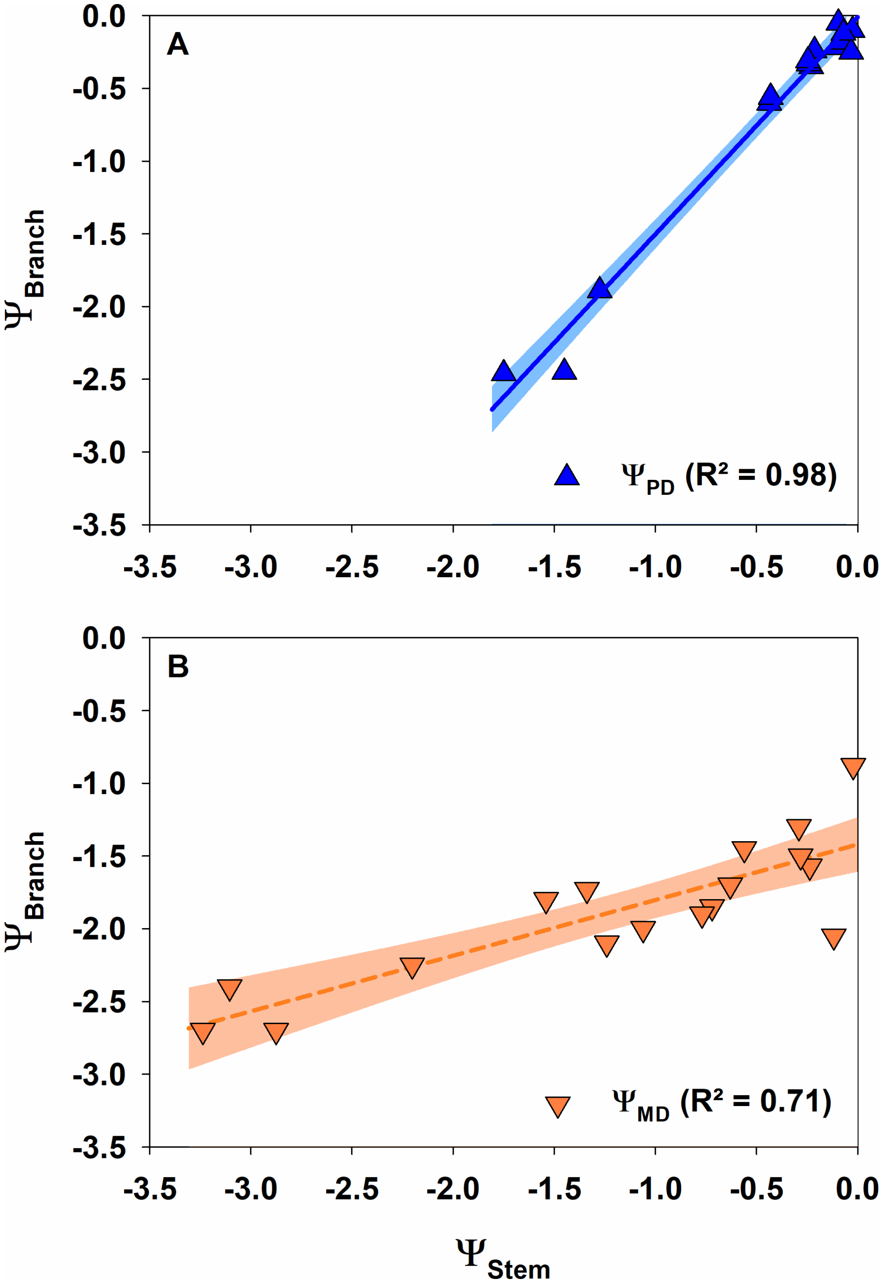

Posted on 26 Aug 2024 — The copyright holder is the author/funder. All rights reserved. No reuse without permission. — https://doi.org/10.22541/au.172471102.26164569/v1 — This is a preprint and has not been peer-reviewed. Data may be preliminary.

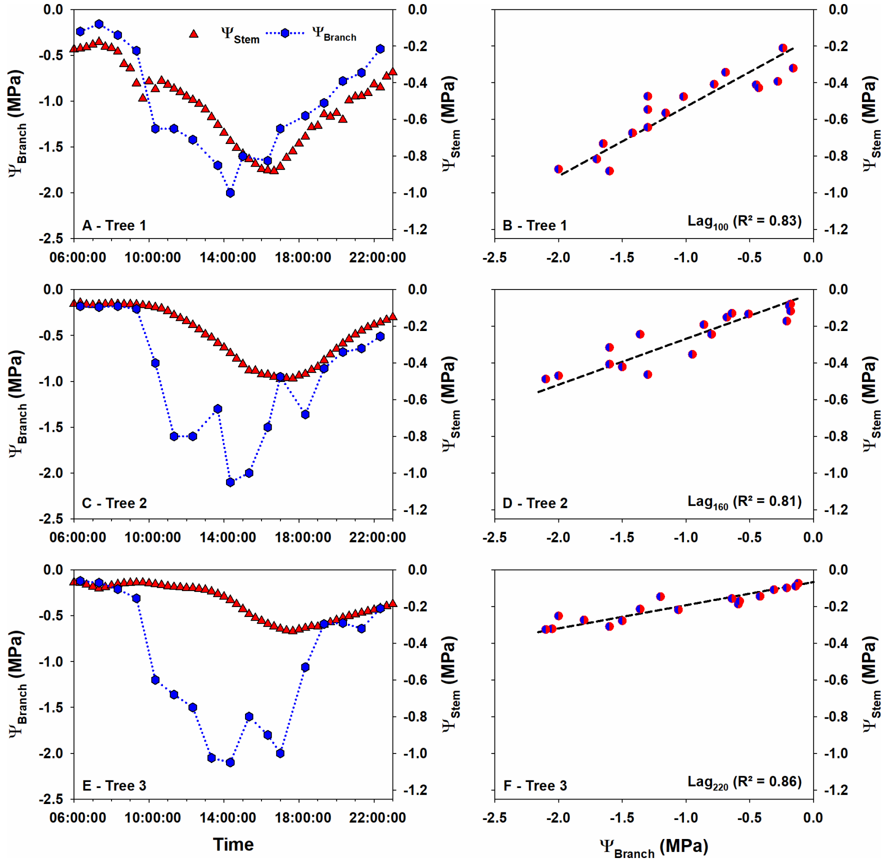

Posted on 26 Aug 2024 — The copyright holder is the author/funder. All rights reserved. No reuse without permission. — https://doi.org/10.22541/au.172471102.26164569/v1 — This is a preprint and has not been peer-reviewed. Data may be preliminary.

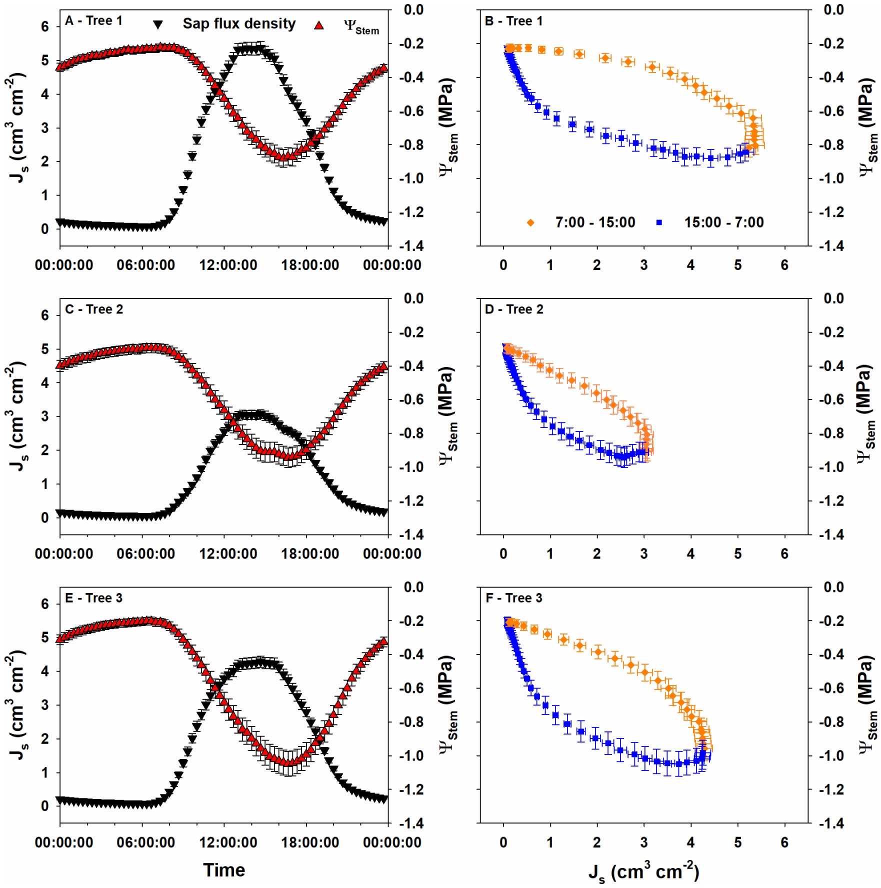

Posted on 26 Aug 2024 — The copyright holder is the author/funder. All rights reserved. No reuse without permission. — https://doi.org/10.22541/au.172471102.26164569/v1 — This is a preprint and has not been peer-reviewed. Data may be preliminary.